How valence bond theory can help you understand your (bio)chemical reaction

4 authors:

A. Shurki
Hebrew University of Jerusalem
50 PUBLICATIONS **1,389** CITATIONS

SEE PROFILE

Etienne Derat
Pierre and Marie Curie University - Paris 6
67 PUBLICATIONS **1,313** CITATIONS

SEE PROFILE

Alexandre Barrozo
University of Southern California
6 PUBLICATIONS **55** CITATIONS

SEE PROFILE

Shina Caroline Lynn Kamerlin
Uppsala University
67 PUBLICATIONS **1,743** CITATIONS

SEE PROFILE

How valence bond theory can help you understand your (bio)chemical reaction†

Avital Shurki,*[a] Etienne Derat,*[b] Alexandre Barrozo[c] and
Shina Caroline Lynn Kamerlin*[c]

Almost a century has passed since valence bond (VB) theory was originally introduced to explain covalent bonding in the H_2 molecule within a quantum mechanical framework. The past century has seen constant improvements in this theory, with no less than two distinct Nobel prizes based on work that is essentially developments in VB theory. Additionally, ongoing advances in both methodology and computational power have greatly expanded the scope of problems that VB theory can address. In this Tutorial Review, we aim to give the reader a solid understanding of the foundations of modern VB theory, using a didactic example of a model S_N2 reaction to illustrate its immediate applications. This will be complemented by examples of challenging problems that at present can only be efficiently addressed by VB-based approaches. Finally, the ongoing importance of VB theory is demonstrated. It is concluded that VB will continue to be a major driving force for chemistry in the century to come.

Key learning points
- Valence bond (VB) theory is a powerful tool to describe (bio)chemical reactivity. It is a vibrant and active research area, with constant developments and improvements.
- VB theory can be generalized into two distinct incarnations: pure *ab initio* VB and its empirical counterpart (EVB).
- The hybrid QM(VB)/MM approach combines *ab initio* VB with molecular mechanics with coupling between the QM and MM which is based on concepts of EVB.
- Developments within the VB field, along with increasing computational power, greatly increase the scope of problems that can be addressed using VB theory.
- The understanding of some key chemical problems, such as hypervalency and charge-shift bonding, can significantly benefit from the framework of valence bond theory.

I. Introduction

In its simplest form, valence bond (VB) theory is used on a daily basis by all chemists around the world. It constitutes the "language" of chemical drawings on a sheet of paper or on a blackboard. Over the past few decades, VB theory has been constantly explored and improved, giving rise to ever more

[a] *Institute for Drug Research, School of Pharmacy, The Hebrew University of Jerusalem, Jerusalem, Israel. E-mail: avitalsh@ekmd.huji.ac.il; Fax: +972 2 675 7076; Tel: +972 2 675 8696*

[b] *Institut Parisien de Chimie Moléculaire, UMR 8232, UPMC – Paris 6, 4 place Jussieu, Paris, France. E-mail: etienne.derat@upmc.fr; Fax: +33 1 4427 7360; Tel: +33 1 4427 3850*

[c] *Science for Life Laboratory, Department of Cell and Molecular Biology, Uppsala University, BMC Box 596, Uppsala, Sweden. E-mail: alexandre.barrozo@icm.uu.se, kamerlin@icm.uu.se; Fax: +46 18 530 396; Tel: +46 18 471 4423*

† Electronic supplementary information (ESI) available: A list of popular simulation packages for performing (E)VB simulations, together with relevant references and download links. See DOI: 10.1039/c4cs00241e

sophisticated approaches grounded in quantum mechanics. This strong resurgence is becoming visible through an explosion of interest in VB approaches as evidenced by the success of meetings such as a VB workshop organized in Paris in 2012, with more than 80 participants,[1] and a second VB workshop, together with the conference "The Chemical Bonds at the 21th Century", as a satellite of the "International Congress of Quantum Chemistry 2015", will be held in June 2015 in Xiamen, China (Information can be found at http://www.cb2015.org/).

VB theory stems from the decomposition of chemical systems into a linear combination of chemically meaningful structures composed of localized orbitals, in contrast to the delocalized orbitals used in molecular orbital (MO) theory. Learning Box 1 illustrates the difference between the approaches. The idea behind VB theory can be traced back to 1927, when Heitler and London came up with a quantitative model, based on quantum mechanics, to explain the covalent bond between the H_2 molecule.[2] This model can be seen as the quantum mechanical version of Lewis electron pair bond theory,[3] in

which the system is described as a linear combination between the electrons occupying each of the hydrogen nuclei. In 1931, Slater and Pauling extended the model to polyatomic molecules, creating the concepts of resonance, hybridization and superposition of covalent and ionic structures (see *e.g.* ref. 4 and references cited therein). These concepts became fundamental pillars of the theory. In the mid 1950s, twenty years later, another significant step was taken towards the establishment of VB theory with Marcus theory of electron transfer,[5] which was awarded the 1992 Nobel Prize in Chemistry. Later, Marcus' work would inspire Warshel to come up with a new VB-based approach to model chemical reactivity, namely the empirical valence bond (EVB) method,[6] which will be described in detail in Section III. This work contributed in part to the award of yet another

Avital Shurki studied chemistry at the Hebrew University of Jerusalem (Israel) and completed her PhD studies of VB as a tool for understanding the structure and reactivity of small molecules under the guidance of Sason Shaik. In 2000 she joined the group of Arieh Warshel at the University of Southern California (Los Angeles, USA) as a post-doctoral fellow and was trying to understand the reactivity of biological systems using the

Avital Shurki

empirical valence bond (EVB) method. In 2003 she joined the School of Pharmacy at the Hebrew University of Jerusalem and developed an ab initio VB/MM method. Her research focuses on the development and application of the valence bond approach to study reactivity in chemistry including both small molecules as well as large biological systems. She is also interested in the development and design of enzymes.

Etienne Derat studied chemistry in Reims (Champagne-Ardennes), followed by a PhD at the same university under the direction of Prof. Stéphane Humbel, working on theoretical organometallic chemistry. In 2004, he started postdoctoral research with Prof. Sason Shaik in Jerusalem on QM/MM and metalloenzymes. In 2006, he became Assistant Professor in the group of Prof. Max Malacria (IPCM-UPMC, Paris). In February 2011, he was an invited professor

Etienne Derat

at the University of Tokyo. He is currently serving as a member of the French National Committee for Research (organic chemistry section). His main field of interest is to understand how large inorganic or organometallic systems evolve by using a broad range of theoretical methods.

Alexandre Barrozo got his bachelor's and master's degrees in physics at the State University of Campinas in 2011, Brazil, where he worked on molecular dynamics simulations for condensed matter systems. He is currently a PhD student at Uppsala University, under the supervision of Dr Shina Caroline Lynn Kamerlin. His work focuses on computational modeling of enzymatic reactions and studying promiscuity among phosphotransferases.

Alexandre Barrozo

Lynn Kamerlin studied Chemistry at the University of Birmingham, where she remained for her PhD studies under the supervision of Dr John Wilkie. This was followed by a short postdoctoral stay at the University of Vienna with Stefan Boresch, as well as a longer postdoctoral stay in the group of Arieh Warshel. In 2011, she was awarded a Junior Researcher grant from the Swedish Research Council (Vetenskapsrådet) to establish her own research

Lynn Kamerlin

group, and she is currently an Associate Professor at Uppsala University. In 2012, she was awarded the Hagbergs Prize in Biochemistry from the Swedish Royal Academy of Sciences; in 2013 she was awarded the MGMS Silver Jubilee Prize from the UK Molecular Graphics and Modeling Society. She is currently an ERC Starting Grantee, a Wallenberg Academy Fellow, and the Chair of the Young Academy of Europe. Her research primarily focuses on the use of valence-bond based approaches to understand the evolution of enzyme function.

Chemistry Nobel prize, this time in 2013 for multiscale modelling. In parallel, other approaches were developed independently, in order to enable calculations that are based on VB concepts. For instance, Goddard and co-workers created the generalized VB (GVB) method,[7] Cooper and coworkers devised the spin-coupled VB (SCVB) approach,[8] and van Lenthe and Balint-Kurti developed a more general multiconfiguration self-consistent field method, the VBSCF method.[9] For a more complete overview of different modern VB methods and their usage, we refer the reader, for example, to the work of Shaik, Hiberty and coworkers.[10,11]

Learning Box 1. Valence bond and molecular orbital theories – two different languages describing the same chemistry
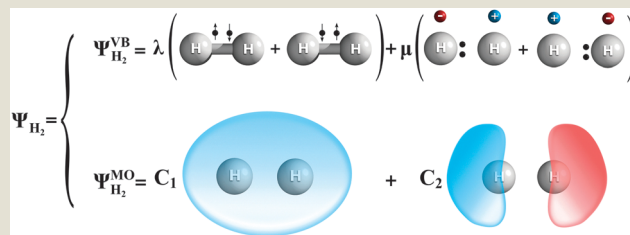
Seen as rivals in the past, VB and MO theories are two ways of describing the same phenomena occurring at the molecular level. While MO theory tries to describe the wavefunctions of electrons as delocalized, by combining all possible atomic orbitals, VB regards the system as a linear combination of possible molecular states, in which the electrons occupy localized orbitals, usually formed by combining only the relevant atomic orbitals. In a quantum mechanical language, as MO looks for the probability of finding electrons at certain points in space, VB looks for the probability of finding a molecule at a given molecular state. The two theories are equivalent and should never be seen as antagonists.

Over the years, most undergraduate students have mainly been taught the simplified version of valence bond theory, while the main focus was on molecular orbital theory. VB theory is, however, a distinct approach that is equivalent to MO theory. That is, VB and MO theories are the two faces of the same coin: a quantum theory of bonding in molecular structures. In some cases (*e.g.* studies of frontier orbitals and electronic transitions), it is less tedious to use the MO approach to reach the desired properties. But for particular cases, VB can be a better methodology despite its greater demands on active involvement by the user and a steeper learning curve. In this review, we will focus on a model S_N2 reaction to guide the readers throughout the practical aspects of using VB theory, as well as illustrating some key applications of this approach. In addition, case studies where VB theory gives more insights than MO theory will also be discussed. The current tutorial review will start by providing a solid theoretical foundation with which to understand modern applications of VB theory. We will follow this by listing and discussing interesting applications of valence bond theory, in order to demonstrate that valence bond theory is (and always has been) an essential tool to analyze the fate of electrons during chemical reactions. The goal of this review will therefore be to provide a generalized understanding of the importance of the field, based on a didactic example that follows the S_N2 like reaction catalyzed by the enzyme haloalkane dehalogenase from the gas-phase through to aqueous solution and finally to the enzyme's active site. This illustrative example demonstrates the power of the VB approach to address all aspects of (bio)chemical reactivity.

II. *Ab initio* valence bond theory

II.1. Valence bond theory – basic concepts

VB theory focuses on the characterization of bonds within molecules. Various VB based approaches have been developed throughout the years (for instance spin coupled VB, GVB, and block localized VB).

In this review we will focus on the original VB approach (see ref. 11 and references cited therein). Its building blocks are VB structures, some of which are equivalent to the well-known Lewis structures. That is, VB theory is based on the idea that the system is described by a collection of structures differing mainly in the composition of the valence electrons. In each VB structure, electrons are associated with particular atoms/fragments and are thus localized to a certain extent. The overall description is a linear combination of the various VB structures formed by different distributions, arrangements and/or pairing of these valence electrons.

The best way to explain the method is by using an illustrative example. The example we have chosen in this work is the S_N2 reaction described in eqn (1).

$$Nu{:}^- + CH_3 - LG \rightarrow Nu - CH_3 + LG{:}^- \tag{1}$$
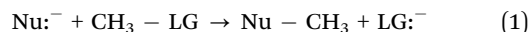
Depending on the identity of the nucleophile (Nu) and the leaving group (LG), the overall number of valence electrons may vary. However, independent of the system, there will always be at least four active electrons, namely electrons that are directly involved in the bond breaking/formation process. These are the C–LG bond electrons and the lone pair electrons of the Nu. To describe the reaction using VB the system will be divided into three fragments, the Nu, the CH_3 group and the LG. Hence, in a simple VB description the four active electrons will be distributed between these three centers (the three fragments). There are six different (independent) ways to distribute and pair four electrons among three centers, leading then to six different VB structures, depicted in Fig. 1A. The electrons are depicted by dots, and the line or line connecting two electrons designates two paired electrons. Thus, for example, placing two electrons on the Nu and one electron on both the CH_3 group and the LG while pairing them results in structure **1**, while placing two electrons on the LG and one electron on both the CH_3 group and the Nu while paring them results in structure **2**, and so forth.

Learning Box 2. Constructing a VB wavefunction

The identity S_N2 reaction $Cl:^- + CH_3Cl$ will serve as an example to illustrate construction of the VB wavefunction. This system involves 22 core electrons (1s, 2s and 2p of Cl and 1s of C), which can be described by MOs and will therefore involve a linear combination of all the system's atomic orbitals (though, in practice, there will only be significant coefficients on the core orbitals). As a result, there will be 11 doubly occupied MOs to describe these 22 electrons. The valence electrons can be divided into active and inactive electrons. Active electrons are those responsible for the different structures, as they are given the freedom to change their occupancy. In the current example these are the two $C{\cdots}Cl_{LG}$ bond electrons and the two electrons of the $Cl_{Nu}:^-$. These four active valence electrons will occupy VB vectors, which will be localized on the corresponding fragments. That is, a linear combination of the atomic orbitals of Cl_{Nu} will form a VB vector that is localized on Cl_{Nu} only and will be occupied by the Cl_{Nu} valence electrons. The same is true for the CH_3 group and the Cl_{LG}, respectively. The remaining inactive electrons will also occupy VB vectors that will be localized on the corresponding fragments. However, depending on the level of calculation, inactive VB vectors with symmetry that differs from that of the active VB vectors may also be delocalized over the whole system. Thus, here the "π inactive" electrons of both Cl atoms and those of the CH_3 group may be either localized on the respective fragments or delocalized over the whole molecule depending on the level of calculation.

Using these VB vectors, the various VB structures can now be constructed. Core electrons and inactive electrons are usually presented by doubly occupied orbitals, which do not differ in the various VB structures. These electrons were omitted from the description. A covalent bond between two electrons in VB vectors φ_1 and φ_2 respectively, presented pictorially by two dots and a connecting line, is described by the Heitler–London wavefunction:[2]

$$\psi_{HL} = \varphi_1(1)\varphi_2(2) + \varphi_2(1)\varphi_1(2)[\alpha(1)\beta(2) - \beta(1)\alpha(2)] = \left|\varphi_1(1)\overline{\varphi_2(2)}\right| - \left|\overline{\varphi_1(1)}\varphi_2(2)\right|$$

Thus, considering only the VB vectors that correspond to the four active electrons, the following equations represent the six different VB structures depicted in Fig. 1:

$$\phi_1 = |\varphi_{Nu}\overline{\varphi_{Nu}}\varphi_C\overline{\varphi_{LG}}| - |\varphi_{Nu}\overline{\varphi_{Nu}}\overline{\varphi_C}\varphi_{LG}| \qquad \phi_4 = |\varphi_{Nu}\varphi_C\overline{\varphi_C\varphi_{LG}}| - |\overline{\varphi_{Nu}}\varphi_C\overline{\varphi_C}\varphi_{LG}|$$
$$\phi_2 = |\varphi_{Nu}\overline{\varphi_C}\varphi_{LG}\overline{\varphi_{LG}}| - |\overline{\varphi_{Nu}}\varphi_C\varphi_{LG}\overline{\varphi_{LG}}| \qquad \phi_5 = |\varphi_C\overline{\varphi_C}\varphi_{LG}\overline{\varphi_{LG}}|$$
$$\phi_3 = |\varphi_{Nu}\overline{\varphi_{Nu}}\varphi_{LG}\overline{\varphi_{LG}}| \qquad\qquad\qquad \phi_6 = |\varphi_{Nu}\overline{\varphi_{Nu}}\varphi_C\overline{\varphi_C}|$$
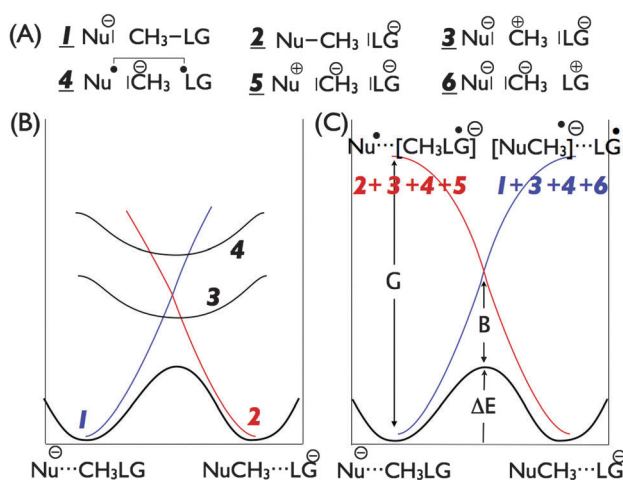

Fig. 1 (A) The six different VB structures (electronic configurations) that describe all possible independent arrangements of four active electrons within the three fragments (Nu, CH_3, and LG). Schematic representation of the VB correlation diagram for the S_N2 reaction described in eqn (1). (B) Using VB configurations describing a general S_N2 reaction (C). Using VB states which are mixtures of selected VB configurations for the particular identity SN2 reaction. Plain lines correspond to the description of the reactant and product structures and states in a and b respectively, and the bold line corresponds to the resulting ground state adiabatic curve.

We note that the advantage of these structures is that they are chemically meaningful. Specifically, structure 1 involves a covalent bond between the LG and the CH_3 group, which is typical of the reactant state, and is therefore often labeled $\Phi_{cov\,R}$. Structure 2 involves a covalent bond between the Nu and the CH_3 group, which is typical of the products state, and is labeled $\Phi_{cov\,P}$. Structure 3 involves negative charge on both the Nu and the LG, while none of these active electrons occupy the

CH_3 group, leading to a positively charged CH_3 group. This structure describes a triple ionic situation and is labeled Φ_{ion1} for brevity. Structure 4 involves a covalent bond between the two distant fragments, Nu and LG, describing a long bond, and is labeled Φ_{LB}. Finally, structures 5 and 6 involve negative charge on both the CH_3 group and the LG or the Nu, respectively, leading the third group to be positively charged. These structures again involve a situation with three charges and are thus labeled Φ_{ion2} and Φ_{ion3}, respectively.

The overall wavefunction of the system within the VB description is therefore a linear combination of these six structures

$$\psi_{VB} = \sum_{i=1}^{N} c_i\phi_i \qquad (2)$$

where ϕ_i is the mathematical representation of the ith structure depicted in Fig. 1, c_i is its respective coefficient in the linear combination and N is the overall number of VB structures (6 in this case). Solving the Schrödinger equation using the variational principle leads to the following set of linear equations

$$\sum_{j=1}^{N} (H_{ij} - ES_{ij})c_j = 0 \qquad i = 1, \ldots, N \qquad (3)$$

where H_{ij} and S_{ij} are the Hamiltonian and overlap matrix elements, respectively, with $H_{ij} = \langle\phi_i|H|\phi_j\rangle$ and $S_{ij} = \langle\phi_i|\phi_j\rangle$. We note in this respect that the diagonal matrix elements of the Hamiltonian, H_{ii}, represent the energy of the corresponding ith structure. That is, in the S_N2 case, for example, H_{11} represents the energy of the covalent structure of the reactants, H_{22} represents the energy of the covalent structure of the products, *etc.* During the reaction, the relative energies of the various structures change along with their contribution to the overall

wavefunction (Fig. 1(B)). ϕ_1, which is $\phi_{\text{cov }R}$ in this example, is relatively stable in the reactant state, and therefore contributes significantly to the wavefunction that describes this part of the reaction. However, as the reaction progresses from reactants to products, the C–LG distance increases and the stabilization of that structure due to the spin pairing of the C–LG bonding electrons is gradually lost. In addition, the Nu–C distance gets shorter and a three-electron repulsion develops. This structure therefore goes up in energy as the reaction proceeds to products. Mixing of all the structures above (also termed diabatic states) results in adiabatic states, the lowest of which describes the reaction profile (bold curve in Fig. 1C). The diagram provides insight into the origin of the barrier formation and was developed into a unified model shown to be useful for both qualitative and quantitative understanding of chemical reactivity.[10,12,13] A detailed interpretation of this diagram will be given in a forthcoming paragraph.

In addition to providing information about the system energy and wavefunction, VB calculations provide additional chemically useful information such as the resonance energy and the weights of the different VB structures. The resonance energy, which is a result of the mixing between the different VB structures, is measured as the difference between the energy of the lowest VB structure, H_{ii}, and the overall ground state energy, E_{g}. The relative weights are derived from population analysis of the overall wavefunction. Hence, there are various different schemes to obtain the relative weights of the different VB structures in the overall wavefunction; eqn (4) presents the Coulson–Chirgwin scheme which is often used (see ref. 11 and 13 and references cited therein):

$$w_i = c_i^2 + \sum_{i \neq j}^N c_i c_j \left\langle \phi_i \mid \phi_j \right\rangle \qquad (4)$$

This additional information, which is not readily available in MO based methods, provides some added value to VB.

II.2. Valence bond theory – how to do it

A common misconception is that VB involves structures but no orbitals. This of course is not correct. Similar to MO theory where the molecular orbitals are a linear combination of atomic orbitals, the VB vectors comprising the VB wavefunction are also a linear combination of atomic orbitals. The difference, however, is that the VB vectors are usually not linear combinations of all the system's atomic orbitals, but rather, each is a linear combination of relevant atomic orbitals which belong to the fragment it describes. We note in this respect, however, that core electrons and sometimes also inactive valence electrons often still utilize orbitals that are equivalent to MOs within the VB description. A detailed example is illustrated in Learning Box 2.

The VBSCF wave function developed by van Lenthe and coworkers[9] consists of all the VB structures of the system described by a common set of orbitals. The orbitals as well as the coefficients of the different structures are optimized simultaneously, leading to a self-consistent field type wave function. Thus, the method is a multi-configuration SCF method with an advantage of utilizing

chemically interpretable configurations. The VBSCF approach was developed both based on the spin free formulation that uses symmetry group methods[14,15] and as a typical multi-configuration spin wave function.[9]

The VBSCF method accounts for static correlation but lacks dynamic correlation. Thus, recent developments involve various *ab initio* VB approaches that incorporate dynamic correlation.[11] These include for example (1) the BOVB, where the average field restriction of the VBSCF is removed and a unique set of orbitals for each VB structure is allowed;[16] (2) the VBCI approach, where the configuration interaction (CI) procedure follows a VBSCF calculation, where replacing occupied VB orbitals by virtual VB orbitals that share the same locality produces excited configurations (see ref. 11 and references cited therein); (3) the VBPT2 approach, which incorporates perturbation theory, where the wavefunction is given as the sum of zeroth-order wavefunction obtained at the VBSCF level and the first-order wavefunction given as a linear combination of the singly and doubly excited structures (see ref. 11 and references cited therein); (4) the DFVB approach, where the density of the VBSCF wavefunction serves, in a self-consistent manner, to determine the correlation functionals and the respective energy is added to the VBSCF energy;[17] and finally (5) the VB/Quantum Monte Carlo approach, where the VB wavefunction is multiplied by a Jastrow factor and a Quantum Monte Carlo calculation is performed.[18]

II.3. Incorporation of solvent effects into valence bond calculations

The methods described thus far relate to small systems in a vacuum. Chemical reactions however often occur in solvents. In these cases one simple way to computationally incorporate the surrounding effect on the reaction is by considering a homogenous solvent with an implicit continuum solvation model. Two VB based methods were developed recently to study chemical reactions in solvents using continuum solvation models: the valence bond polarizable continuum model (VBPCM) (see ref. 19 and references cited therein) and the VB solvent model (VBSM) which combines VB with parameters determined for the SM6 solvation model.[20]

The VBPCM level combines the VB approach with the polarizable continuum model. Here, the interactions between the solute charges and the polarized electric field of the solvent are considered by embedding an interaction potential in the quantum Hamiltonian:

$$\left(H^0 + V_{\text{R}}\right)\Psi^{\text{VB}} = E\Psi^{\text{VB}} \qquad (5)$$

VBSM on the other hand utilizes the implicit solvent model SM_X (currently $X = 6$) to account for the solvation of the solute of interest.[20] The electrostatic interactions between the solvent and the solute within the SM6 model are described by the generalized born (GB) approximation with self-consistent solute charges (see ref. 20 and references cited therein). The solvation free energy, ΔG_{s}, in this model is composed of the following terms

$$\Delta G_{\text{s}} = \Delta E_{\text{E}} + G_{\text{p}} + G_{\text{CDS}} \qquad (6)$$

where ΔE_E is the difference in the expectation value of the gas-phase Hamiltonian for the solvent-phase wavefunction and the gas-phase wavefunction, G_p is the free energy due to the polarization of the solvent by the solute charges and G_{CDS} is the free energy term that accounts for cavitation, dispersion and solvent structure. These methods, however, consider the environment as being homogenous, and are therefore not suitable to describe reactions in biological systems where the fine details of the structure are usually responsible for the observed reactivity. Section III will discuss far more consistent fully microscopic approaches for describing solvent in VB calculations, and it is also worth mentioning here the semi-microscopic approach introduced in ref. 6, which already at an early stage introduced the solvation in the diagonal VB states, an approach which captures most of the solvent effect. An added advantage of moving to a fully microscopic description of the solvent is that it is possible to take into account effects such as non-equilibrium solvation.

II.4. Quantitative results using valence bond theory

In this paragraph, results obtained by quantitative valence bond calculations on a prototypical S_N2 reaction in aqueous solution will be described. Such calculations were done using both the VBPCM[19] and the VBSM methods.[20] Here we will elaborate on the former. One of the simplest S_N2 reactions that can be imagined is the replacement of a chloride by another chloride in a single methyl group. The starting structure is obviously a chloride anion approaching methyl chloride (structure **1** in Fig. 1) and the product is the symmetrical structure (structure **2** in Fig. 1). But, since valence bond theory allows one to express the wave-function as a superposition of various structures, one can add other electronic descriptions of the chemical system. The reagent can thus be described by a superposition of structures **1**, **3**, **4** and **6**: in **3**, the bond between carbon and its chloride is considered as fully ionic with a positively charged carbon atom; in **6**, the same bond is again fully ionic but with a positively charged chlorine atom and finally in structure **4**, the two electrons of the chloride anion are split between the two chlorine atoms giving rise to a long bond between them. In the product, structures **1** and **6** are replaced by their symmetrical counterparts structures **2** and **5**.

Using this set of structures, one can perform VBPCM calculations at the VBSCF level (VBPCM//VBSCF) as explained before. The experimental value for this chloride exchange is known to be 26.5 kcal mol^{-1}. The calculated VBPCM//VBSCF/6-31G* value is found to be 36.1 kcal mol^{-1}, a clear-cut overestimation of the barrier. Is there a problem in describing this simple reaction within Born–Oppenheimer approximation? It seems not, since the CCSD(T) value with the same basis set is 28.6 kcal mol^{-1}. One can nevertheless still notice the 2 kcal mol^{-1} error margin, which is slightly above the "golden standard" for chemical accuracy in quantum chemistry (≤ 1 kcal mol^{-1}). Therefore, what is wrong with the VBSCF calculation, when including the effect of solvation? During the VBSCF optimization, the canonical orbitals remain identical for all the sets of VB structures, which is obviously wrong since a cation has more contracted orbitals than an anion. Since the S_N2 reaction is dealing with charged species, allowing the set of structures to re-adapt their canonical

orbitals is mandatory for obtaining reasonable energetic values, in the so-called BOVB framework. This is indeed the case since the VBPCM//BOVB/6-31G* value for the chloride exchange is found to be 26.8 kcal mol^{-1}. Thus, in this particular case, BOVB outperforms the CCSD(T) level by one order of magnitude.

If energetic values are usually the main quantitative value emerging from MO calculations, VB calculations also allow one to easily retrieve the weight of the various structures. Fig. 1 shows the six structures used in the VBPCM//BOVB/6-31G* calculations and it is thus possible to gain access to their relative weights on the critical points of the potential energy surface. Since the reagent and product are the same in this identity reaction, only two points will be discussed here, the RS and the TS as shown in Table 1.

For the minimum, the main structure is, as expected, the first one (labeled **1** in Fig. 1) with a relative weight of 64%. The second most important structure is the one for which the carbon is positively charged, *i.e.* structure **3** with a weight of 26%. Structure **6**, with one positively charged chlorine atom accounts for 10% of the weighting. The contributions from the other structures are negligible. At the transition state (TS), the relative weight of the structures is modified: the weight of structure **3**, the one with a carbon-centered cation, is increasing from 26% to 49% reflecting the planarization of the carbon during chlorine exchange. On the other hand, structures **1** and **2** are equalized (at 24%), which sounds logical taking into account the symmetrical shape of the TS. Finally the long bond structure weight (**4**) is non-negligible at the TS with a weight of 3%, showing that spin-pairing can occur across the carbon centre, facilitating electronic reorganization.

Now that the BOVB calculations have established the electronic components of the S_N2 reaction, it is possible to build a valence-bond state correlation diagram (VBSCD) from this.[10,12,13] This diagram is shown in Fig. 1C. The bold line represents the adiabatic state resulting from the mixing of all the configurations (**1** to **6**). But one can also extract the states corresponding respectively to the reagent and the product (**1**, **3**, **4**, **6** and **2**, **3**, **4**, **5**). Diabatic curves for the reagent and product rise continuously from their respective minimum and correlate with their respective charge-transfer state ($Cl^\bullet \cdots CH_3Cl^-$, where structure **4** mixes to shift the extra electron in the CH_3Cl species). This also explains the increased weight of structure **4** at the TS. The two curves cross in the middle of the diagram. At this crossing point, the diabatic curves mix to generate the ground state of the TS. Since the charge-transfer state is a key component of the S_N2 reaction, it seems natural to include the related parameter into the diagram: this is the gap (G) between the ground state and the charge-transfer state. Another key component is the mixing

Table 1 Weights of VB structures **1–6** for the reactant and transition state of the identity S_N2 reaction in the aqueous solution[a]

	1	**2**	**3**	**4**	**5**	**6**
RS	0.640	0.000	0.263	0.000	0.000	0.097
TS	0.239	0.239	0.488	0.029	0.003	0.003

[a] Results are obtained at the VBPCM//BOVB/6-31G* level of theory. The corresponding structures are shown in Fig. 1.

occurring at the TS (usually called resonance in the framework of the VB theory). It is indicated by B in Fig. 1C. All these components taken together allow the barrier height to be determined by a linear relationship, which is given by

$$\Delta E^{\ddagger} = fG - B \tag{7}$$

where f is the fraction of the gap. For the chloride exchange exemplified here, one can find that the gap is 222 kcal mol^{-1} with a fraction of 0.2 and resonance energy of 17 kcal mol^{-1}, which gives 27 kcal mol^{-1} for the barrier determined before. A similar treatment can be done for other halogen exchange reactions.

Learning Box 3. EVB is a QM/MM method

The EVB approach uses the classical free energy perturbation/umbrella sampling (FEP/US) procedure, with the difference that bonds that are formed and cleaved are described by a Morse potential. The quantum mechanical behavior arises from the fact that we are mixing all the reactants, intermediates and product states, and the energies of the system are obtained by calculating the eigenvalues of the relevant quantum mechanical Hamiltonian matrix. In the example we are using, the calculation is performed in the same way as a two-level quantum system (a general treatment can be found in any quantum mechanics textbook). The coupling of the parabolas is determined by a set of semi-empirical parameters, which will position one of them using the other as a reference. Therefore, this is identical to any semi-empirical approach that replaces the integral with empirical functions, with the exception that the VB rather than MO formalism is being used.
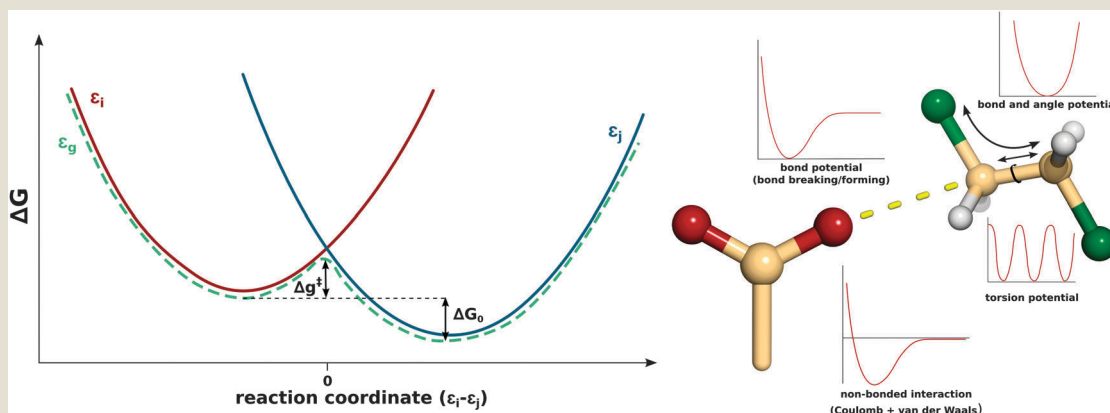
III. The empirical valence bond approach

III.1. EVB – basic concepts

Despite significant advances in computational power, the use of higher-level quantum mechanical approaches remains cumbersome for complex (bio)chemical systems, particularly if one is interested in obtaining convergent free energies. This problem is circumvented by the empirical incarnation of valence bond theory,[21] which is a semi-empirical QM/MM method that uses fully classical descriptions of different key stationary points within a quantum mechanical framework in order to be able to describe bond-breaking and bond-making processes. The advantages of this approach are that it is fast, allowing for extensive conformational sampling, while carrying a tremendous amount of chemical information, allowing for a physically and quantitatively meaningful description of chemical reactivity.[22]

As within a standard VB framework, a chemical reaction is described as a combination of classical VB states, although the focus is on different potential bonding patterns highlighted in Fig. 1C and less attention is paid to the different electronic configurations highlighted in Fig. 1A and B. These different VB states are described by curved energy surfaces, obtained using classical force field description, as illustrated in Learning Box 3. Each VB state in an EVB description corresponds to different

bonding patterns of key energy minima (reactants, products and any intermediates) along the postulated reaction coordinate. Here, the use of Morse rather than harmonic potentials to describe changing bonds allows for these bonds to eventually be broken. However, left to their own devices, the timescales of such bond transformations are well out of the league of current simulation approaches. Hence, the actual chemical reaction is described using a mapping potential that is a linear combination of these different diabatic states, using empirical parameters to describe the coupling between these parabolas, as will be outlined below (note as an aside that unlike the VB approach described in Section II, in the EVB approach the states are chosen in a way that there is zero overlap between them). The EVB approach thus takes into account the resonance of these different structures in the same way that quantum states are mixed in any quantum system, and the energies along the reaction coordinate are obtained like in every quantum-mechanical problem, by looking for the eigenvalues of the Schrödinger equation for the mixing of the different states. These eigenvalues are obtained by diagonalizing the energy matrix for this system, and, once these values are obtained, it is possible to generate the relevant adiabatic free energy profile.

The EVB approach relies on calibration of empirical parameters to describe the energetics of a reference reaction (either in vacuum or in solution, or even a wild-type enzyme, if one is interested in a range of mutants). Once calibrated, those parameters can be used

to describe the same process in a different environment, such as an enzyme active site. They characterize the coupling between the curved surfaces shown in Learning Box 3. The way the EVB approach is structured allows one to directly compare how the presence of a different electrostatic environment affects the energetics of the studied reaction, since one maintains the same parameterization for the reacting atoms and only changes the environment (while treating the QM/MM coupling between the solute and the environment consistently). In addition to its direct empirical implementation, the EVB approach can also be used as a reference potential to account for the environment effects, allowing calculations of free energy to be performed efficiently for both *ab initio* QM/MM[23] as well as for frozen/constrained DFT calculations.[24] Another advantage of the EVB approach (as any other VB based method) is that it can handle challenging charge separation reactions properly and consistently reproduce the catalytic effect of many enzymes with high accuracy.[25] Furthermore, the approach is able to correctly reproduce the linear free energy relationship between activation free energies and their corresponding reaction free energies,[22] and has also played a key role in showing that electrostatics is the major factor in driving enzyme catalysis.[25]

III.2. EVB in practice – the haloalkane dehalogenase reaction

Section II illustrated the use of VB theory to describe a more generalized S_N2 reaction. Here, we will follow the reaction catalyzed by haloalkane dehalogenase from the gas phase through to aqueous solution and finally to the enzyme's active site. This enzyme converts haloalkanes into primary alcohols using a catalytic triad (Asp124, Asp260 and His289), with the carboxylic group of Asp124 acting as the nucleophile.[26] In its simplest form,

the relevant reacting atoms are the whole 1,2-dichloroethane substrate and the nucleophilic carboxylate group, as shown in Fig. 2. Since EVB provides relative rather than absolute energies, it is necessary to have a reference state to which to fit the EVB parabola. This is often taken to be the background reaction in aqueous solution, as biology occurs in aqueous solution, but can also be the corresponding reaction in vacuum or the wild-type enzyme relative to a range of mutants. When using a model reaction, amino acid side chains involved in the reaction are normally truncated to the closest chemical counterpart, for example acetate or propionate to describe an aspartic acid, imidazole to describe histidine and so forth. The background reaction is then fit to either direct or extrapolated experimental data, or, if necessary, to higher level quantum chemical calculations. In this particular case, it is possible to use known values of a reaction that is close enough to the reference reaction in order to estimate the activation barrier using acetic acid as a model for the nucleophilic Asp124.[26]

In order to start building the parabolas describing the reaction, we need to define how the Hamiltonian (energies) of the system will look like, so we can construct the relevant energy matrix. Let us start with the simplest case: the gas-phase reaction. Here the environmental effects are not yet a challenge. The diagonal elements of the Hamiltonian matrix, which correspond to the average energy for each state, are described by

$$H_{ii} = \varepsilon_{ii} = U_{qq}^i(\mathbf{R},\mathbf{Q}) + \alpha_{gas}^i \tag{8}$$

Here, $\mathbf{R}$ and $\mathbf{Q}$ are vectors representing the atomic coordinates and charges of all the elements of a given state i (1 for the reactant state, and 2 for the product state, see Fig. 2 and Learning Box 3), U_{qq}^i is the potential energy of interaction within the atoms participating in the chemical reaction (q),
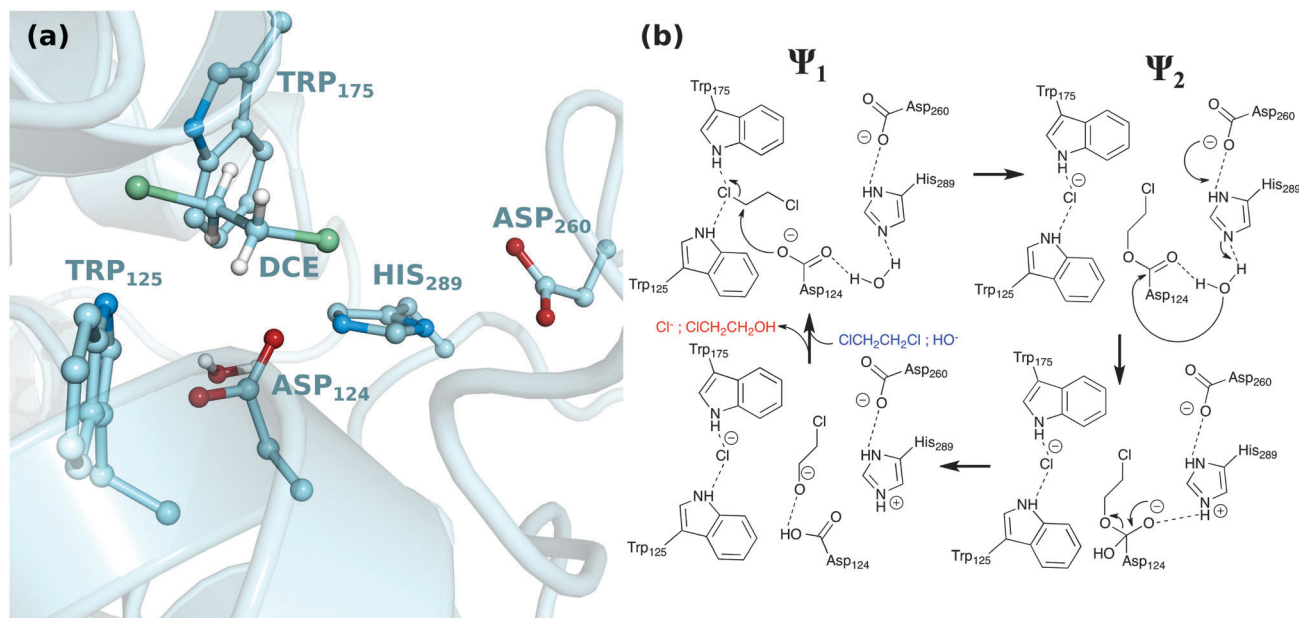

Fig. 2 (a) An overview of the haloalkane dehalogenase (DhlA) active site (based on the structure PDB code 2HDC and highlighting key active site residues). (b) A schematic overview of the S_N2 mechanism catalysed by DhlA showing the involvement of the residues highlighted in (a) in the chemical mechanism. The "Ψ_1" and "Ψ_2" highlighted in part B correspond to the two reacting states considered in the EVB calculations discussed in Section III.

including the electrostatic energy, van der Waals interactions, and the covalent bond, angle and torsion energies, and α_{gas}^i is the gas-phase energy of the ith state, representing the energy difference between both fragments at infinite separation. For the off-diagonal elements H_{ij}, which are related to the superposition of the diabatic surfaces corresponding to the different EVB states, this can be represented by simple exponential functions (although more complex functions could also be used if necessary):

$$H_{ij} = A \exp[-\mu(r - r_0)] \tag{9}$$

In the expression above, r represents the distances between relevant reacting atoms (in this specific case, the nucleophilic O from the carboxylic group and the electrophilic C from the substrate), considered with respect to the equilibrium distance r_0, and A and μ are constants. The choice of such a function reflects the decay in coupling of the states with distance. With these definitions set, our Hamiltonian matrix will be

$$H = \begin{pmatrix} \varepsilon_1 & H_{12} \\ H_{21} & \varepsilon_2 \end{pmatrix} \tag{10}$$

The ground state energy of our system can then be obtained by diagonalizing this matrix.

Since we are interested in analyzing the free energy profile for the whole reaction, we have to explore all the possible geometrical configurations of the system going from the reactant to the product state under a given reaction coordinate x. Therefore, the procedure for obtaining the ground state energy stated above should be used along many different configurations, which includes sampling unstable parts of the reaction, which is the case for the TS. To achieve this, we use a standard free energy perturbation/umbrella sampling (FEP/US) procedure.[21,27] In this method, we create artificial states alongside the reaction pathway, using a linear combination of the energies of the diabatic states. For the case of two states, we would have

$$\varepsilon_m = (1 - \lambda_m)\varepsilon_1 + \lambda_m\varepsilon_2 \tag{11}$$

where λ_m is a mapping parameter going from 0 to 1 in a number of fixed increments ($\lambda_m = 0, 1/N, 2/N,\ldots, N/N$). Each of these steps will yield configurations at different points in the reaction coordinate (here defined as the energy gap between the two diabatic states, $x = \varepsilon_1 - \varepsilon_2$). The energy gap reaction coordinate is a particularly powerful reaction coordinate to represent multidimensional conformational space, as it allows for a description of the environmental reorganization along the reaction coordinate without being biased by the choice of pre-defined geometric variables. This in turn allows for more efficient sampling. The free energy between steps m and n, $\Delta g_{m,n}$, can be calculated by using eqn (12)

$$\Delta g_{m,n}(x') = \sum_{i=m}^{n-1} -\beta^{-1} \ln\langle\delta(x - x')\exp\{-\beta[\varepsilon_{i+1}(x) - \varepsilon_i(x)]\}\rangle_{\varepsilon_i} \tag{12}$$

and the accumulated contributions from each step in the whole process will give the desired free energy profile. The Dirac delta
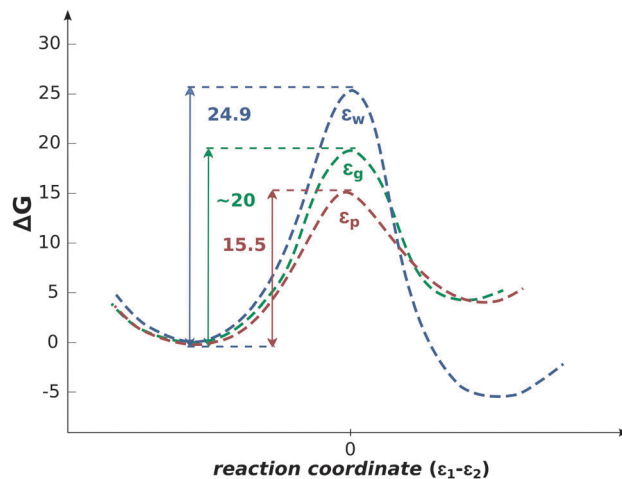

Fig. 3 A comparison of schematic EVB free energy profiles for the reaction catalysed by haloalkane dehalogenase (DhlA, Fig. 2), obtained in the gas-phase (ε_g), aqueous solution (ε_w) and in the enzyme active site (ε_p). See also discussion in the main text.

in eqn (12) represents the fact that the reaction coordinate, x, will be restricted to the configurations that correspond to the mapping potential ε_m. By using several discrete steps, it will be possible to make the complete mapping of the gas-phase free energy profile, highlighted in Fig. 3.

Now let us consider the effect of the environment where the reaction takes place. The only important change will come at eqn (8), in which the energies will now become

$$H_{ii} = \varepsilon_i = U_{qq}^{ii}(\mathbf{R},\mathbf{Q}) + U_{pq}^i(\mathbf{R},\mathbf{Q},\mathbf{r},\mathbf{q}) + U_{pp}^i(\mathbf{r},\mathbf{q}) + \alpha_{gas}^i \tag{13}$$

where we have the interaction between the reacting fragments and the atoms of the environment (p, with atomic coordinates $\mathbf{r}$ and charges $\mathbf{q}$), as well as the interaction among all the environment atoms within themselves. Note that the gas-phase shift has been demonstrated to be phase-independent, and rigorous constrained DFT (CDFT) calculations have shown that the off-diagonal elements remain the same for any electrostatic environment.[28] This is a powerful feature of the EVB approach, as it allows one to model the same chemical reaction in distinct chemical environments, using the same gas-phase shift and off-diagonal values, and thus directly observe how changing the environment affects the reaction. It should be pointed out that α_{gas} can, in principle, be applied to either of the diabatic states to either raise or lower the energy of the relevant parabola. However, irrespective of which state is chosen, once the reaction has been calibrated in one environment, it is absolutely crucial to apply it to the same state consistently.

As a final note, some readers might be concerned about the precision of using a semi-empirical force field based approach to describe the energies of the different diabatic states. While this approach is generally quite useful as the parabolas have been rigorously parameterized, it is nevertheless worth mentioning that the accuracy of the EVB approach can be dramatically improved by (mostly) automated fitting to higher level quantum chemical potentials, or even by just using it as a classical

reference potential. These are now more advanced concepts that are worth mentioning, but rather than discussing it in detail here, we refer interested readers to ref. 29 and references cited therein.

III.3. EVB – quantitative results

As seen in the previous section, the EVB approach is a powerful method to analyze the contribution of the environment to a chemical reaction and therefore understand the molecular basis for chemical catalysis. Here, we will present some sample results from EVB studies on the reaction catalyzed by haloalkane dehalogenase (DhlA), in the enzyme and in the background reaction. These studies were performed in order to analyze the catalytic effect of this system, with the aim of identifying the source of the catalytic proficiency of the enzyme.[26]

As in every EVB study, one has to parameterize the empirical parameters by fitting the energies of a reference reaction to known or estimated kinetic data. In the case of DhlA, the reaction involves nucleophilic attack by a carboxylate ion on chloromethane. The model reaction used in this work was the S_N2 reaction $CH_3COO^- + CH_3Cl \rightarrow CH_3COOCH_3 + Cl^-$. The choice of formate rather than an aspartate to mimic the Asp124 nucleophile in this reference reaction does not affect substantially the calculation of the activation barrier (see footnote 68 in ref. 26). Due to the lack of available experimental data on this reaction, the authors were forced to calibrate their EVB parameters as carefully as possible to experimental data on analogous reactions, obtaining an estimate of ~ 27 kcal mol^{-1} for the activation barrier of the background reaction. Based on this calibration, the authors were able to obtain an activation barrier of 15.2 kcal mol^{-1} for the reaction in the DhlA active site, which is very close to the experimental value of 15.3 kcal mol^{-1} (ref. 26) (see also Fig. 3).

The main point of this work was to use EVB to analyze what the principal factors driving catalysis by this enzyme are. One of the strong features of the method lies in its ability to probe the intersection between the different electronic states. With the aid of linear response approximation (LRA) treatment, it is possible to decompose free energies into individual contributions.[30] The EVB energy surface itself allows one to obtain relevant structures of reactant and transition states, and these can be properly sampled by means of molecular dynamics simulations. Olsson and Warshel[26] used this feature and calculated the free energy of solvation for the two states by applying the LRA analysis. The idea here was to show that catalysis is not driven by desolvation (or reactant state destabilization). Instead, the enzyme acts as a "super solvent", providing better TS stabilization than in the corresponding uncatalyzed reaction in aqueous solution. This is due to the fact that the enzyme has an electrostatic environment that is preorganized to solvate the reacting fragments, in contrast to the background reaction in which the solvent dipoles have to reorganize in order to properly solvate the polarized TS. In both cases, this reorganization has an energetic penalty, which is substantially smaller in enzyme than in solution. Using the LRA approach, coupled with rigorous EVB simulations, the authors were able to quantify this reorganization

penalty in both environments, demonstrating that it is 12 kcal mol^{-1} higher in the background reaction than in the electrostatically preorganized environment of the DhlA active site. This difference in fact accounts for nearly all the catalysis provided by DhlA, a phenomenon that has been seen across a broad range of enzymes.[25]

IV. Combined *ab initio* VB/MM calculations

IV.1. Basic concepts and practical considerations

As will be seen in Section V, valence bond theory is a conceptual tool that is particularly efficient at describing the nature of bonding in various chemical systems. Thus, it seems natural to also adapt it when addressing bigger systems such as the ones commonly encountered in biology. Classical approaches are well suited for modeling enzymes (or other biological macromolecules) due to their extensive sizes. However, such methods are intrinsically limited by the fact that they cannot deal with electron reorganization. In order to integrate the best of both worlds, a solution is to simultaneously perform classical and quantum mechanical calculations, a methodology coined under the term QM/MM and first developed by Warshel and Levitt.[31] An example of this is the EVB approach described in Section III, which is an empirically-based QM/MM approach that uses VB concepts to describe reactions in biomolecules. Although one can, in principle, have an unlimited number of VB states, due to the calibration requirement, EVB can be easily applied only when there are a limited number of VB states (commonly two) involved. In addition, while powerful, for such calculations to be physically meaningful, they are dependent on the accuracy of the force field used and they require extensive parameterization of the quantum region. Consequently, in some cases, it might be necessary to move to a more numerically precise description of the quantum region.

From a technical point of view, two main directions have been developed for performing QM/MM calculations. One of these is called an additive scheme, and one is called a subtractive scheme (with ONIOM being its best representative). The distinction between these two approaches is in the way in which the coupling between the QM and MM regions is treated. Specifically, in an additive scheme, the QM energy including MM polarization is added to the MM energy, whereas in a subtractive scheme, the difference between the high and low levels in the inner system is added to the energy of the full system at the low level. Also one needs to ideally consider polarization effects. This, in turn, leads to three distinct approaches to address this issue. The first of these is the simplest, in which the QM and MM parts do not polarize each other, and only mechanical embedding is taken into account. In the second approach, the MM point charges polarize the QM region in a process referred to as electrostatic embedding. In the final approach, there is cross-polarization between the MM $\rightarrow$ QM regions, as in the previous case, and the QM region has an impact on the MM atoms (which is normally a polarizable

force field in that particular situation). In the case of *ab initio* VB calculations, this issue has been overcome by a framework that combines the additive scheme with polarization of the QM region by the empirical force field.[32] The total Hamiltonian can thus simply be written as

$$H_{\text{VB/MM}} = H_{\text{VB}} + H_{\text{MM}} + H_{\text{VB-MM}} \qquad (14)$$

These three terms designate the valence bond Hamiltonian of the reactive part, the molecular mechanics Hamiltonian of the surroundings and the coupling Hamiltonian between the reactive part and the surroundings, respectively. Since the

polarization of the QM region by the MM part is incorporated, the third term, defining the coupling part of the Hamiltonian, is described as follows:

$$H_{\text{VB-MM},ii} = H_{ii}^{\text{int}} \qquad (15)$$

$$H_{\text{VB-MM},ij} = \tfrac{1}{2}(H_{ii}^{\text{int}} + H_{jj}^{\text{int}})S_{ij} \qquad (16)$$

where H_{ii}^{int} is the interaction of the reactive part with the environment in the ith VB structure calculated classically; and S_{ij} is the overlap between the ith and jth VB structures calculated in vacuum.

Learning Box 4. Reduced resonance integral *vs.* off diagonal element

Empirically it was established that the resonance energy, B, is a value that is intrinsic to the reaction, and hence does not depend on the environment. B, as shown in Fig. 1C, is the difference between the energy of the most stable VB structure (H_{ii}), and the total system energy (E_{total}). Using some simple algebra, one can show that for a 2×2 VB system, the resonance energy at the crossing point between the two VB states (B in Fig. 1C) is given by $B = (H_{12} - H_{11}S_{12})/(1 + S_{12})$. Since the energy of the two states is equal at the crossing point (*i.e.* $H_{11} = H_{22}$), it can be given by the average of the two states, leading to $B = (H_{12} - (1/2)(H_{11} + H_{22})S_{12})/(1 + S_{12})$. In the empirical VB framework (EVB), the overlap S_{12} is assumed to be zero, hence $B = H_{12}$ and the assumption of invariance of B to the environment transforms into invariance of the off-diagonal term, H_{12}. In the *ab initio* VB framework on the other hand (*e.g.*, VB/MM), a value that is often used is the reduced resonance integral β_{ij}. This integral, which is given by $\beta_{ij} = H_{ij} - 1/2(H_{ii} + H_{jj})S_{ij}$, is the same as that used by simple MO models such as the extended Hückel theory. It is easy to show that the resonance energy B is given by $B = \beta_{12}/(1 + S_{12})$ and the assumption of invariance of B to the environment in the VB/MM framework therefore transforms into invariance of both the overlap and the reduced resonance integral.

The main idea is to consider the external environment of the MM part as a perturbation on the VB structures, affecting each VB structure differently, as well as the interaction between the different VB structures. Adjunction of these different interactions to the various matrix elements and solving the Hamiltonian through a variational process ensure polarization of the overall wavefunction.

Eqn (16) is based on the assumption that both the overlap and the reduced resonance between VB structures do not depend on the environment. This assumption is equivalent to the assumption made in the EVB approach regarding the off-diagonal element. It was shown to be usually justified.[28,33] For clarification of the relation between the off-diagonal term and the reduced resonance integral see Learning Box 4. Extension of the method which involves calculating the electrostatic interactions with the environment using the electrostatic embedding approach led to the density embedded VB/MM (DE–VB/MM) method.[34] Here, none of the assumptions described above is required to calculate the electrostatic effect of the environment on the reactive part of the system, as the point charges of the atoms describing the environment are introduced in the core Hamiltonian of the quantum part. This DE–VB/MM approach, however, is computationally more demanding than the standard VB/MM. Hence for most applications VB/MM, despite its use of approximations, can serve as the first method of choice.[33,35,36]

IV.2. VB/MM – quantitative results

In principle, the VB/MM approach has all the capabilities of the *ab initio* VB methods described in Section II. Therefore, for continuity, we will start as previously with the example of the identity S_N2 reaction to illustrate the results that can be obtained through VB/MM calculations. More specifically, comparison with previous methods such as VBSCF (BOVB) and

VBPCM will be highlighted. Once again, since the reaction is identical, the same set of valence bond structures can be used (Fig. 1A): the covalent ones (**1** and **2**), the long-bond structure (**4**) and the ionic ones (**3**, **5**, and **6**). To simplify the calculations, only structures **1**, **2** and **3** were used in the VB/MM scheme, eliminating structures **4**, **5** and **6**, the contributions from which were shown to be negligible. From an energetic point of view, the quantitative results obtained are pretty good. For example, while the experimental barrier for the exchange of chloride anion is known to be 26.5 kcal mol⁻¹, VB/MM calculations found a value of 26.0 kcal mol⁻¹.[33]

Concerning the relative weighting of the VB structures, what emerges from a comparison of the VBSCF and VB/MM results is a remarkable stability of the relative weights despite the inclusion of specific solvation (Fig. 4). It shows that the qualitative picture of the S_N2 reaction was already captured by gas-phase calculations. One can nevertheless notice an increase of the ionic weight for the solvated transition state, which sounds logical since the covalent structures are gaining less solvation at the transition state.

Non-equilibrium solvation effects that could not be accounted for by the continuum models (*e.g.* VBPCM) can be calculated using the VB/MM approach, as it involves an explicit solvent description. This involves, for example, the charge transfer gap (G in Fig. 1C and eqn (7)), which is one of the parameters that controls the barrier height following the VBSCD model of Shaik and co-workers.[10,12,13] This value was calculated to be only 222 kcal mol⁻¹ using the VBPCM, which is closer to the 194 kcal mol⁻¹ value calculated in a vacuum than to the estimated value ($\geq$281 kcal mol⁻¹) in solution and is a result of the absence of non-equilibrium solvation effects required to calculate the promoted state.[19] Using VB/MM where explicit water molecules are considered, such effects are now
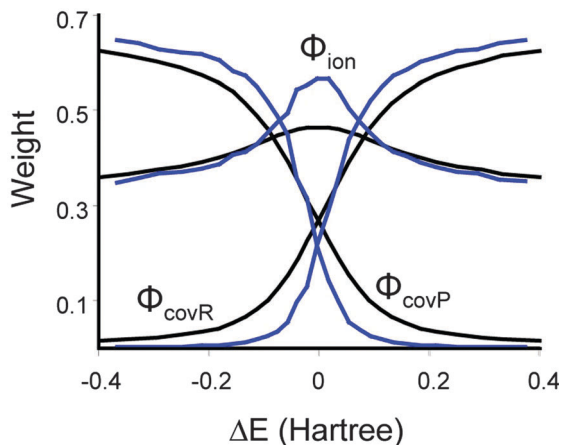
Fig. 4 Weights of the 3 major VB configurations (**1**, **2** and **3**) that compose the overall wave function of the identity S_N2 reaction discussed in Fig. 1. Gas-phase weights are in black and weights in solution calculated with the VB/MM method are in blue.

accounted for and the value is estimated to be 324 kcal mol^{-1}.[36] We note in this respect that this value is probably overestimated mainly due to technical issues, including for example, the fact that quantitatively, the picture obtained in the calculations is not as simplistic as in the qualitative model. The real value is therefore somewhere between the estimation (≥ 281 kcal mol^{-1}) and the calculated one (324 kcal mol^{-1}).

The advantage of the VB/MM approach is that it can also be applied to study enzymes. Hence, similar to the EVB we will next illustrate it on the reaction catalyzed by haloalkane dehalogenase. Here, the VB structures are again those defined in Fig. 1A where now the Nu is Asp124 modelled by propanoate in the QM part of the calculation, and the LG is the leaving chloride anion (see also Fig. 2a). In this system the quantum part is covalently linked to the environment. This is done using the link atom scheme where a link atom (hydrogen in this case) is used in the QM calculation to cap the dangling bonds and saturate their free valency (see *e.g.* ref. 35 and references cited therein).

The VB/MM energy is then calculated. When we are interested in analyzing the free energy profile for the whole reaction, similar to the EVB, we have to explore all the possible configurations of the system going from the reactant to the product state. However, due to the high computational cost, and the current lack of gradient calculations within *ab initio* VB, this is done using the potential of mean force combined with FEP.[27]

The VB/MM catalytic effect in this reaction was calculated to be 8.2 kcal mol^{-1}, which is again in reasonable agreement with the estimated experimental value of ~ 11 kcal mol^{-1}.[26] The reaction energetics can be analyzed in terms of contributions of the VB configurations. Such analysis is done using the LRA procedure, as outlined in Section III.[30] In this particular case, for example, the solvation of the different configurations was calculated. It was shown that water stabilizes the covalent structure (structure **1**) in the reactant's geometry much more than in the TS (54 *vs.* 17 kcal mol^{-1}, respectively). This difference in the stabilization of structure **1** leads therefore to

the high barrier. This result is in agreement with the organic chemist's explanation for the increased barrier in polar solvents, stabilizing the RS more than the TS in this particular system. In the protein on the other hand, the protein dipoles do not change much, and this differential solvation is much smaller, leading in turn to a smaller barrier.[35]

V. Some applications of *ab initio* and empirical valence bond theory to solving (bio)molecular problems

V.1. 1,3-Dipolar cycloadditions

1,3-Dipolar cycloadditions have attracted a lot of interest recently due to their ability to generate an adduct starting from two components, leading to so-called "click" chemistry. The two components are, respectively, the 1,3-dipole and the dipolarophile (Fig. 5) While the dipolarophile is a classical alkene or alkyne, the 1,3-dipole has an electronic structure which can be described by the superposition of three valence bond structures (Fig. 5(a)). Structure A can be described as a propargyl, structure B as an allenyl, while structure C involves two unpaired electrons.

The problem associated with this reaction arises from the fact that barriers are found to be similar whatever the dipolarophile is. By using the classical approach of frontier molecular orbitals (Fig. 5(b)), one should obtain different barriers, since the HOMO and LUMO of ethene and ethyne are not of the same energies. 1,3-Cycloaddition is thus an example of a reaction unexpectedly not following frontier molecular orbital theory. Investigations were undertaken using VB theory to decipher the reasons behind these contradictory results.[37]

BOVB calculations on a series of dipolarophiles enable access to the weighting of the different structures A, B, and C. It appears that the ionic structures A and B represent roughly 75% of the system, while the diradical structure C accounts for 25% of the system. This value is non-negligible, and it is even more significant when taking into account the distorted geometry of the cycloaddition transition state. In that case, the weighting of the structure increases to roughly 35%. Distortion of the 1,3-dipole is thus the key event that allows the reaction to take place. Moreover the calculations suggest that the role of the distortion is to modify the electronic state of the 1,3-dipole in order to make it more reactive, and thus it explains why identical distortions (and barriers) are expected for additions to ethylene and acetylene, which are in fact observed. Finally, a linear correlation between the diradical character of 1,3-dipoles and the barrier height was found, explaining the intriguing fact that the barrier heights for the cycloaddition of a given 1,3-dipole to acetylene and ethylene are very similar, despite the difference in exothermicity. In summary, what emerges from VB calculations on this particular topic is the fact that increasing the diradical character is the driving force of the 1,3-cycloaddition.

V.2. Hypervalency and charge-shift bonding

Charge-shift bonding has emerged as a new type of bond on the basis of valence bond calculations and analysis. Usually, bonding
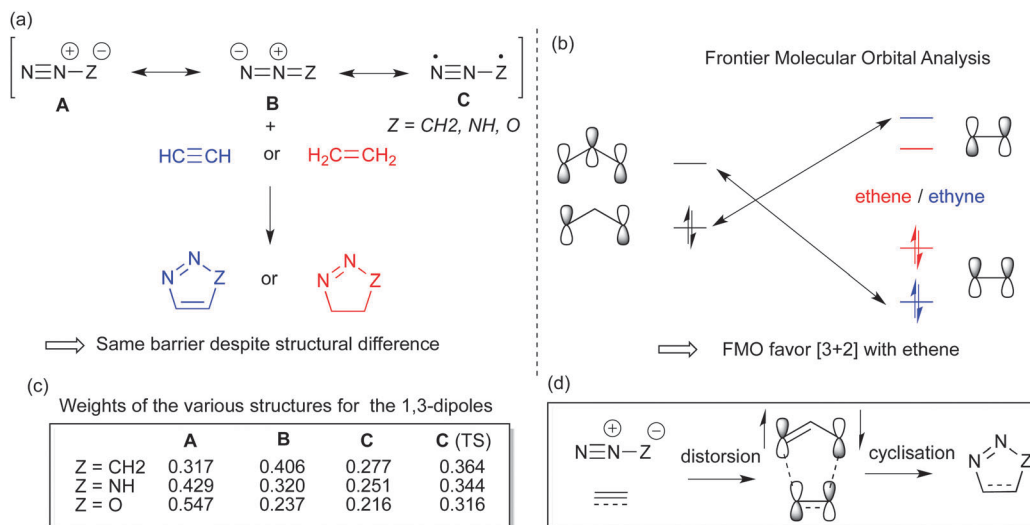
Fig. 5 (a) Schematic illustration of a 1,3-dipolar cycloaddition, (b) simplified frontier molecular orbital analysis, (c) BOVB based weighting of the VB structures of various 1,3-dipoles,[37] and (d) the proposed mechanism as deduced by valence bond theory.

in the molecular structure is divided into two families: covalent and ionic. In the framework of valence bond theory, this splitting is somewhat formal since the global electronic structure is described as a superposition of covalent and ionic structures. But VB allows a definition of covalent or ionic bonds by establishing what the dominant contribution among the various substructures is. Examining the energetic contribution of the dominant VB structure has challenged this idealized picture. For example, in a simple molecule like F_2, the dominant VB structure is the covalent one but at the equilibrium distance its energetic contribution is destabilizing.[38] In fact, the bonding energy in such situation is arising from the mixing between the covalent and ionic structures, and is physically due to an increase in the charge fluctuation.

To highlight this charge-shift concept, the bonding pattern of XeF_2 will now be examined.[39] XeF_2 is a typical hypervalent molecule, which can be described through the Rundle–Pimentel model, *i.e.* a three-center-four-electron molecular orbital diagram. To describe this model in terms of a VB framework, one can also use three main structures as depicted in Fig. 6. The first of these is a set of two symmetrical structures with one covalent bond between xenon and fluorine and an ionic bond between xenon and the opposite fluorine (structures D and E in Fig. 6, notice that the d orbital can also be used on the central atom); the second of these is a structure where Xe is neutral while the two fluorine atoms share two paired electrons giving rise to a long bond between them (structure F) and the last of these is a structure involving two ionic bonds between the central atom and its ligand (structure G). It is interesting to notice that these structures resemble the ones used for describing the S_N2 reaction.

In Fig. 6 are also indicated the energies of the various VB structures (or combinations of them in the D and E cases) for XeF_2 relative to atoms at infinite separation. It appears that the four structures taken separately cannot account for the stability of this hypervalent molecule. Mixing structures D and E leads to
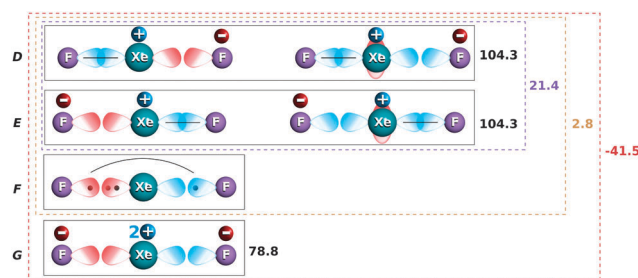

Fig. 6 VB structures for XeF_2, as well as the energies of the corresponding diabatic states (in kcal mol^{-1}).

a more stable energetic configuration (21.4 kcal mol^{-1}), which, however, is still repulsive relative to the atoms at infinite separation. Including the long-bond structure F allows one to reach a value close to zero; but the stability of XeF_2 is only explained by mixing all four structures. This shows that the bonding energy is due to a large resonance between the various structures enabled by a strong covalent–ionic mixing. This is a typical case of charge-shift bonding. In summary, VB theory has shown that many chemical bonds, including hypervalency, should be described by the mixing of covalent and ionic VB structures, and their actual bond strength is dictated by the corresponding covalent–ionic resonance energies. This charge shift bonding concept has helped increase our understanding of various intriguing bonding and reactivity problems, including for example the inverted bond in [1.1.1] propellane and the rarity of ionic chemistry of silicon in the condensed phase.[40,41]

V.3. Quadruple bonding in C_2 and its isoelectronic molecules

An additional novel yet intriguing insight from modern VB methods is, for example, the quadruple bonding in C_2 and its analogues (Fig. 7).[42]
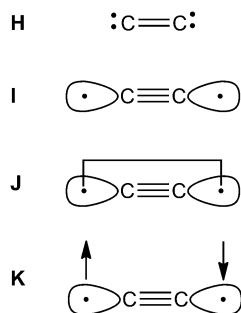
Fig. 7 Three possible bonding schemes of the C_2 molecule (H, I, and J), and the quasi-classical state of the fourth bond, K (for details, see discussion in the main text).

Fig. 8 Calculated energy landscape for ATP hydrolysis by F_1-ATPase, as a function of both the rotary motion of the system (x-axis) and the chemical step (y-axis). This shows that the catalytic dwell of the system upon 80° rotation is to allow for the chemical step to occur. Reproduced with permission from ref. 45.

The bond order of diatomic molecules with eight-valence electrons using the simple molecular orbital diagram is two, as in structure H (Fig. 7), because of the electron occupation of both $2\sigma_g$ and $2\sigma_u$, which leaves only the contribution of the 4π electrons to the bond order. The same molecules described with simple sp-hybridization are considered to have a bond order of three, as in I, with one σ and two π bonds leaving one electron on each atom pointing away from the bond. VB methods, however, show that these outwardly pointing electrons form an inverted bond, leading to a bond order of four (J in Fig. 7).

The strength of the fourth bond was assessed within the VB framework, by calculating the *in situ* bond energy, which is the bonding interaction of that fourth bond within the molecule. This can be estimated by the difference between the energy of the molecule and the molecule where this bond is in its non-bonding, quasi-classical state (K, which is one of the spin arrangements of the covalent structure). Alternatively, this bond energy can be estimated as half the gap between the singlet and triplet states of that molecule. The different approaches resulted in bond strengths of >10 kcal mol^{-1} suggesting that this fourth bond is rather weak, yet not negligible. This study inspired other researchers and opened a debate regarding the nature of the bonding in C_2 and its analogues.[43,44] Nevertheless, it emphasizes the unique capabilities of modern VB.

V.4. Modeling large biomacromolecules with EVB calculations and simplified models: the case of ATP synthase

It is well known that high-level quantum chemical calculations are computationally very expensive. When it comes to studying the dynamical behavior of enzymes, one has to deal with thousands of atoms, since the whole protein network is of vital importance for the catalytic effect. Moreover, it is important to properly include the electrostatic effects of the environment where the turnover takes place, in order to calculate free energies of chemical reactions in a meaningful way. Thus, the use of hybrid QM/MM methods becomes necessary, and the EVB is one of the most efficient methods available for studying large systems due to a combination of both its speed and accuracy. This approach has been extensively used to study the catalytic effect of a large number of enzymes.[25]
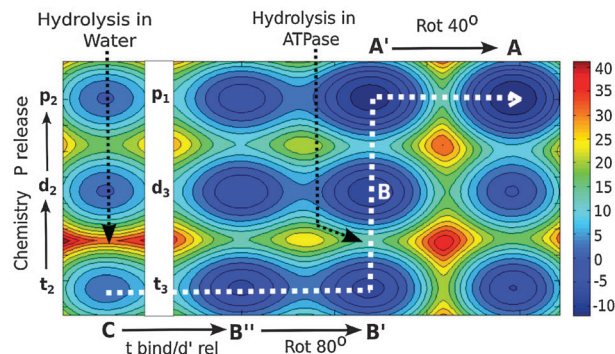
A remarkable example of the power of the EVB approach can be seen in a series of studies by Warshel and co-workers on the energetics of the F_0/F_1-ATPase systems (Fig. 8).[45–47] In the case of F_1-ATPase, the system has over 23.000 atoms and couples major conformational changes to the catalytic effect within its active site. In the authors' first work,[47] EVB calculations were performed on this system with the objective of obtaining the activation barriers for the synthesis of ATP inside the dimeric units of F_1-ATPase. As for any EVB procedure, that work dealt with a reference reaction to calibrate the empirical parameters for the underlying turnover. The EVB calculations were then performed with 31 frames of 5 ps each for both the reference and the enzyme reactions. These calculations allowed for a reproduction of the catalytic effect of the enzyme within 1 kcal mol^{-1} of precision for this challenging system.

In the next work,[45] the authors explored the relationship between the energy barrier for the hydrolysis of ATP and the conformational changes in the enzyme (Fig. 8). Here, the authors showed a clear coupling between the conformational motion of the enzyme and how the reaction takes place. Specifically, by following the conformational/catalytic landscape, the authors observed that the step of hydrolysis must occur at a very specific conformation of the whole complex, in which the dimer which holds the ATP is rotated 80° before the hydrolysis takes place This is essentially a least free energy pathway, since EVB calculations for different conformations other than the one stated above yield a higher free energy pathway, as shown in Fig. 8. Additionally, by coupling the EVB free energy surface with free energy surfaces associated with the conformational changes, the authors could explain the curious catalytic "dwell" in different conformations,[48] in which the F_1-ATPase spends most of its time of hydrolysis at the very conformation used for the catalysis. The authors again managed to reproduce the chemical barrier to within 1–2 kcal mol^{-1} of precision compared to experiment.

Finally, in a following work,[46] the authors sought to map the free energy profile behind the mechanical rotation of the F_0-ATPase, which is the rotary motor of the whole ATPase.

The article shows that the asymmetry in the energetics of the proton path is an important factor for performing the torque on the c-ring component. In this case, EVB was used as a tool to generate an electrostatic profile for the proton transport, which was later used for studying the dynamical aspects of the rotation of the molecular machine. Here we see an example of the use of EVB as a source of chemically relevant free energy profiles to study biological phenomena other than enzymatic catalysis.

VI. Conclusions

In this tutorial review, we have presented a range of methods that utilize VB concepts to study reactivity within chemistry. Various applications that emphasize the added value and insights gained by using VB based methods have also been presented. We note that there are many additional VB based methods, not discussed in this review, that are either derived from the methods described here or constitute similar developments. For a wider review of the various methods the reader is referred to ref. 11, 49 and 50. Additionally, a list of popular simulation packages for performing (E)VB simulations is provided as ESI.†

Historically, full application of the fantastic capabilities of *ab initio* VB methods to any system has often been limited by computer resources. Thus, the continuous current growth in computational power guarantees great future developments in that field. In parallel, the ability to do increasingly long-timescale VB simulations using empirical methods has increased their popularity in the field, in particular when combined with their relative ease of use and the wealth and variety of problems that are and can be solved. Finally, the development of the VB/MM, which relies on both worlds, is expected to bridge the gap, combine the benefits from both worlds and further augment potential problems, the solution of which within the VB framework is feasible. Such developments will greatly contribute to advances in the reactivity of both small molecules as well as biological systems and play a major role in computational (bio)chemistry in the decades to come, while maintaining the beauty of VB: its ability to simplify without being simplistic.

Acknowledgements

Notes and references

1 B. Braïda, E. Derat, S. Humbel, P. C. Hiberty and S. Shaik, *ChemPhysChem*, 2012, **13**, 4029–4030.
2 W. Heitler and F. London, *Z. Phys.*, 1927, **44**, 455–472.
3 G. N. Lewis, *J. Am. Chem. Soc.*, 1916, **38**, 762–785.
4 J. C. Slater, *Phys. Rev.*, 1931, **37**, 481–489.
5 R. A. Marcus, *Annu. Rev. Phys. Chem*, 1964, **15**, 155–196.
6 A. Warshel and R. M. Weiss, *J. Am. Chem. Soc.*, 1980, **102**, 6218–6226.
7 W. A. Goddard, T. H. Dunning, W. J. Hunt and P. J. Hay, *Acc. Chem. Res.*, 1973, **6**, 368–376.
8 D. L. Cooper, J. Gerratt and M. Raimondi, *Chem. Rev.*, 1991, **91**, 929–964.
9 J. H. van Lenthe and G. G. Balint-Kurti, *J. Chem. Phys.*, 1983, **78**, 5699–5713.
10 S. Shaik and P. C. Hiberty, *Rev. Comput. Chem.*, 2004, **20**, 1–100.
11 W. Wu, P. F. Su, S. Shaik and P. C. Hiberty, *Chem. Rev.*, 2011, **111**, 7557–7593.
12 S. Shaik and A. Shurki, *Angew. Chem., Int. Ed.*, 1999, **38**, 586–625.
13 S. Shaik and P. C. Hiberty, *A chemist's guide to valence bond theory*, John Wiley & Sons, New Jersey, 2008.
14 R. Mcweeny, *Int. J. Quantum Chem.*, 1988, **34**, 25–36.
15 L. C. Song, Y. R. Mo, Q. N. Zhang and W. Wu, *J. Comput. Chem.*, 2005, **26**, 514–521.
16 P. C. Hiberty, J. P. Flament and E. Noizet, *Chem. Phys. Lett.*, 1992, **189**, 259–265.
17 F. M. Ying, P. F. Su, Z. H. Chen, S. Shaik and W. Wu, *J. Chem. Theory Comput.*, 2012, **8**, 1608–1615.
18 B. Braïda, J. Toulouse, M. Caffarel and C. J. Umrigar, *J. Chem. Phys.*, 2011, **134**, 084108.
19 L. C. Song, W. Wu, P. C. Hiberty and S. Shaik, *Chem. – Eur. J.*, 2006, **12**, 7458–7466.
20 P. F. Su, W. Wu, C. P. Kelly, C. J. Cramer and D. G. Truhlar, *J. Phys. Chem. A*, 2008, **112**, 12761–12768.
21 A. Warshel, *Computer Modeling of Chemical Reactions in Enzymes and Solutions*, Wiley-Interscience, USA, 1997.
22 S. C. L. Kamerlin and A. Warshel, *WIREs Comput. Mol. Sci.*, 2011, **1**, 30–45.
23 N. V. Plotnikov, S. C. L. Kamerlin and A. Warshel, *J. Phys. Chem. B*, 2011, **115**, 7950–7962.
24 T. Wesolowski, R. P. Muller and A. Warshel, *J. Phys. Chem.*, 1996, **100**, 15444–15449.
25 A. Warshel, P. K. Sharma, M. Kato, Y. Xiang, H. B. Liu and M. H. M. Olsson, *Chem. Rev.*, 2006, **106**, 3210–3235.
26 M. H. M. Olsson and A. Warshel, *J. Am. Chem. Soc.*, 2004, **126**, 15167–15179.
27 M. E. Tuckerman, *Statistical Mechanics: Theory and Molecular Simulation*, Oxford University Press, USA, 2010.
28 G. Y. Hong, E. Rosta and A. Warshel, *J. Phys. Chem. B*, 2006, **110**, 19570–19574.
29 N. V. Plotnikov, *J. Chem. Theory Comput.*, 2014, **10**, 2987–3001.
30 Y. Y. Sham, Z. T. Chu, H. Tao and A. Warshel, *Proteins: Struct., Funct., Genet.*, 2000, **39**, 393–407.
31 A. Warshel and M. Levitt, *J. Mol. Biol.*, 1976, **103**, 227–249.
32 A. Shurki and H. A. Crown, *J. Phys. Chem. B*, 2005, **109**, 23638–23644.
33 A. Sharir-Ivry and A. Shurki, *J. Phys. Chem. B*, 2008, **112**, 12491–12497.
34 A. Sharir-Ivry, H. A. Crown, W. Wu and A. Shurki, *J. Phys. Chem. A*, 2008, **112**, 2489–2496.

35 A. Sharir-Ivry, T. Shnerb, M. Štrajbl and A. Shurki, *J. Phys. Chem. B*, 2010, **114**, 2212–2218.

36 A. Sharir-Ivry and A. Shurki, *J. Phys. Chem. A*, 2008, **112**, 13157–13163.

37 B. Braïda, C. Walter, B. Engels and P. C. Hiberty, *J. Am. Chem. Soc.*, 2010, **132**, 7631–7637.

38 S. Shaik, P. Maitre, G. Sini and P. C. Hiberty, *J. Am. Chem. Soc.*, 1992, **114**, 7861–7866.

39 B. Braïda and P. C. Hiberty, *Nat. Chem.*, 2013, **5**, 417–422.

40 A. Shurki, P. C. Hiberty and S. Shaik, *J. Am. Chem. Soc.*, 1999, **121**, 822–834.

41 S. Shaik, D. Danovich, W. Wu and P. C. Hiberty, *Nat. Chem.*, 2009, **1**, 443–449.

42 S. Shaik, D. Danovich, W. Wu, P. F. Su, H. S. Rzepa and P. C. Hiberty, *Nat. Chem.*, 2012, **4**, 195–200.

43 G. Frenking and M. Hermann, *Angew. Chem., Int. Ed.*, 2013, **52**, 2–6.

44 S. Shaik, H. S. Rzepa and R. Hoffman, *Angew. Chem., Int. Ed.*, 2012, **52**, 3020–3033.

45 S. Mukherjee and A. Warshel, *Proc. Natl. Acad. Sci. U. S. A.*, 2011, **108**, 20550–20555.

46 S. Mukherjee and A. Warshel, *Proc. Natl. Acad. Sci. U. S. A.*, 2012, **109**, 14876–14881.

47 M. Štrajbl, A. Shurki and A. Warshel, *Proc. Natl. Acad. Sci. U. S. A.*, 2003, **100**, 14834–14839.

48 H. Ueno, T. Suzuki, K. Kinosita and M. Yoshida, *Proc. Natl. Acad. Sci. U. S. A.*, 2005, **102**, 1333–1338.

49 A. Warshel and J. Florián, *Encyclopedia of Computational Chemistry*, 2004.

50 A. Shurki and A. Sharir-Ivry, *Isr. J. Chem.*, 2014, **54**, 1189–1204.